AIP | Journal of Applied Physics

Charge states of the reactants in the hydrogen passivation of interstitial iron in P-type crystalline silicon

Chang Sun, AnYao Liu, Sieu Pheng Phang, Fiacre E. Rougieux, and Daniel Macdonald

Citation: Journal of Applied Physics **118**, 085709 (2015); doi: 10.1063/1.4929757
View online: http://dx.doi.org/10.1063/1.4929757
View Table of Contents: http://scitation.aip.org/content/aip/journal/jap/118/8?ver=pdfcov
Published by the AIP Publishing

Articles you may be interested in

Evidence for an iron-hydrogen complex in p-type silicon
Appl. Phys. Lett. **107**, 032103 (2015); 10.1063/1.4927323

Hydrogen passivation of interstitial iron in boron-doped multicrystalline silicon during annealing
J. Appl. Phys. **116**, 194902 (2014); 10.1063/1.4901831

Precipitation of iron in multicrystalline silicon during annealing
J. Appl. Phys. **115**, 114901 (2014); 10.1063/1.4868587

Precipitates and hydrogen passivation at crystal defects in n - and p -type multicrystalline silicon
J. Appl. Phys. **102**, 093702 (2007); 10.1063/1.2800271

Interactions of B dopant atoms and Si interstitials with SiO 2 films during annealing for ultra-shallow junction formation
J. Appl. Phys. **97**, 073520 (2005); 10.1063/1.1884246

APL Photonics is pleased to announce Benjamin Eggleton as its Editor-in-Chief

[This article is copyrighted as indicated in the article. Reuse of AIP content is subject to the terms at: http://scitation.aip.org/termsconditions. Downloaded to] IP: 130.56.107.4 On: Wed, 28 Oct 2015 23:41:13

CrossMark click for updates

Charge states of the reactants in the hydrogen passivation of interstitial iron in P-type crystalline silicon

Chang Sun,[a)] AnYao Liu, Sieu Pheng Phang, Fiacre E. Rougieux, and Daniel Macdonald
Research School of Engineering, College of Engineering and Computer Science, The Australian National University, Canberra, ACT 2601, Australia

(Received 24 July 2015; accepted 17 August 2015; published online 31 August 2015)

Significant reductions in interstitial iron (Fe_i) concentrations occur during annealing Fe-containing silicon wafers with silicon nitride films in the temperature range of 250 °C–700 °C. The silicon nitride films are known to release hydrogen during the annealing step. However, in co-annealed samples with silicon oxide films, which are hydrogen-lean, changes in the Fe_i concentrations were much less significant. The precipitation of Fe_i is ruled out as a possible explanation for the significant reductions. The hydrogen passivation of Fe_i, which is the complexing of monatomic H and isolated Fe_i forming a recombination-inactive hydride, is proposed as the most probable model to explain the reductions. Under the assumption that the reduction is caused by the hydrogenation of Fe_i, the reactants' charge states in the hydrogenation reaction are determined by two independent approaches. In the first approach, illumination is found to have a small but detectible impact on the reaction kinetics in the lower temperature range. The dominating reactants' charge states are concluded to be $Fe^0 + H^+$ as revealed by modelling the injection-dependent charge states of isolated Fe_i and monatomic H. In the second approach, the reaction kinetics are fitted with the Arrhenius equation over a large temperature range of 250 °C–700 °C. A reasonable fit is only obtained when assuming the reacting charge states are $Fe^0 + H^+$. This supports the conclusion on the reacting charge states and also gives a value of the activation energy of hydrogenation in the 0.7–0.8 eV range. © *2015 AIP Publishing LLC*. [http://dx.doi.org/10.1063/1.4929757]

I. INTRODUCTION

Fe is one of the most common metallic impurities in photovoltaic grade crystalline silicon.[1] Previous studies have shown the total Fe concentration in photovoltaic multicrystalline silicon wafers can be in the 10^{14}–10^{15} cm^{-3} range, with 10^{11}–10^{13} cm^{-3} being in the dissolved interstitial state.[2,3] Both Fe_i and Fe precipitates can significantly reduce the carrier lifetime.[1] External gettering is a common and effective method to remove Fe_i from the bulk of silicon wafers during cell fabrication.[4] There is also the possibility to reduce the impact of Fe_i via hydrogenation. Several previous studies reported a reduction in [Fe_i] or in the recombination activity of Fe-related traps after the incorporation of hydrogen into the silicon bulk, by hydrogen ion implantation[5] or simply by annealing a hydrogenated silicon nitride passivation film on the wafer surface.[6–8] The authors have attributed this reduction to the hydrogenation of Fe_i. Some of the authors proposed that the hydrogenation reaction is the binding of H and Fe_i atoms, forming a recombination-inactive hydride.[5,8] In the recent study by Liu *et al.*,[8] it was shown that the observed reduction of Fe_i is unlikely to be caused by internal gettering by crystallographic defects, which may be accelerated by the enhanced diffusivity of Fe_i in the presence of hydrogen, as has been proposed elsewhere.[9,10]

As a closely related topic on the hydrogenation of defects in silicon, the boron-oxygen (BO) defect and its permanent deactivation have been studied in recent years.[11–26] It has been shown that the permanent deactivation of the defect, which occurs under illumination at elevated temperatures, appears to require the presence of hydrogen.[13–21,25] In some studies, the permanent deactivation is explained by the significant change of the charge states of monatomic hydrogen under illumination, which accelerates the hydrogen passivation of the defect.[15,18–20,23,25] Similarly, in the possible hydrogenation of Fe_i, it is also probable that only Fe and H atoms in certain charge states participate in the reaction. In some reports, it has been conjectured that the paring reaction is driven by the Coulombic attraction between Fe^+ and H^-, but this has not been proven experimentally.[8,23]

As predicted in a recent model for charge states of defects in silicon, at a lower temperature range (300 °C and below), carrier injection has a significant impact on the charge distributions on the energy levels of Fe_i and H.[23] Assuming different reacting charge states, the presence of carrier injection therefore affects the hydrogenation reaction. This provides a theoretical basis for the experimental determination of the charge states of the reactants. In this work, we measure the kinetics of the hydrogenation of Fe_i in p-Si at the lower temperature range, both in the dark and under illumination. We model the charge states of Fe_i and H as a function of both temperature and injection level by applying a general charge occupancy factor, as described in Ref. 23. The charge states of the reactants are then determined by combining the experimental and modelling results. We then measure the kinetics of the hydrogenation reaction in the dark across a higher temperature range from 300 °C to

a)Electronic mail: chang.sun@anu.edu.au.

 © 2015 AIP Publishing LLC

[This article is copyrighted as indicated in the article. Reuse of AIP content is subject to the terms at: http://scitation.aip.org/termsconditions. Downloaded to] IP: 130.56.107.4 On: Wed, 28 Oct 2015 23:41:13

700 °C and estimate the activation energy of hydrogenation, using a more complete reaction rate model.

II. EXPERIMENTS

The samples in this study were Float-Zone (FZ) boron-doped silicon wafers. The doping of the samples was in the $8.0–8.5 \times 10^{15}\,\mathrm{cm}^{-3}$ range, determined by dark conductance. The wafers were chemically etched to remove the saw damage, resulting in thicknesses between 260 and 270 μm. Then, they were implanted with 70 eV Fe^{56} ions to doses of $3.0 \times 10^{11}\,\mathrm{cm}^{-2}$ and $5.2 \times 10^{10}\,\mathrm{cm}^{-2}$. After implantation, the samples were cleaned and annealed at 1000 °C in dry oxygen for 45 min, and in nitrogen for 30 min, followed by cooling down to 750 °C with a cooling rate of 10 °C/s and then cooled down rapidly to room temperature in air. This process allowed the implanted Fe atoms to distribute uniformly throughout the thickness of the wafers and froze them in the interstitial state, as well as growing SiO_2 films providing surface passivation. Some of the wafers were then dipped in diluted hydrofluoric acid solution to remove the oxide film and were passivated with Plasma-Enhanced Chemical Vapor Deposited (PECVD) SiN_x films, deposited in a Roth and Rau AK400 chamber. The set temperature of the PECVD reactor was 450 °C, but the actual temperature of the samples during the deposition was about 250 °C. The thickness of the SiN_x film on each side of the sample was about 80 nm.

In this work, we hydrogenated Fe_i by annealing the samples with SiN_x films, which served as the hydrogen source upon annealing. The samples with SiO_2 films served as control samples, as the oxide films contain virtually no hydrogen. The injection-dependent lifetime was measured with the Quasi-Steady-State Photo-Conductance (QSSPC) technique.[27,28] The concentration of Fe_i ([Fe_i]) was measured by applying the FeB pair dissociation method described in Ref. 29. The recombination parameters of isolated Fe_i and FeB pairs at room temperature are taken from Ref. 30.

Two sets of experiments were then conducted. The first set of experiments was performed at 250 °C and 300 °C on the samples with the lower implantation dose, to check the impact of illumination during annealing. The samples with lower dose were chosen because they had higher lifetimes, so that higher injection levels could be achieved under illumination. At each temperature of 250 °C and 300 °C, a sample with SiN_x films and a sample with SiO_2 films were annealed on a hotplate in the dark, and another sample with SiN_x films was annealed on the hotplate under illumination by a xenon white lamp with a constant intensity. The illumination intensity was about 50 suns (1 sun = 100 mW/cm^2, assuming the spectrum is similar to AM1.5G spectrum), measured by a reference cell. The [Fe_i] as a function of cumulative annealing time was measured on each sample. The data from this set of experiments were then used to determine the reactants' charge states in the hydrogenation, as described below.

The other set of experiments was conducted in the temperature range of 300 °C–700 °C, on the samples with the higher implantation dose, to obtain more data for the estimation of the activation energy. At each temperature of 300 °C, 400 °C, and 500 °C, a sample with SiN_x films and a sample with SiO_2 films were annealed on the hotplate in the dark. An additional sample with SiN_x films was annealed at 500 °C. For this sample, we stripped off the annealed nitride film and put on a new nitride film every time before measuring [Fe_i], to check the effect of re-passivation at this temperature. At each temperature of 600 °C and 700 °C, a sample with SiN_x films and a sample with SiO_2 films were annealed in a Rapid Thermal Processor (RTP). The samples were annealed in between two other silicon wafers with similar sizes to block the illumination in the RTP. The samples with nitride films were re-passivated every time before measuring [Fe_i]. Again for all the samples, we measured [Fe_i] as a function of cumulative annealing time.

III. MODELLING PROCEDURE

A. Charge states of isolated Fe_i and monatomic H

The hydrogenation of Fe_i is assumed to be a first-order reaction with respect to Fe and H.[31] Under this assumption, the reaction rate will linearly depend on the concentration of each reactant according to the law of mass action. Assuming the charge states of the reacting Fe atom and H atom are x and y, the reaction can be written as

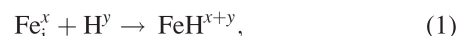

$$Fe_i^x + H^y \rightarrow FeH^{x+y}, \quad (1)$$

where x can be 0/+ and y can be +/0/−. Table I lists all the possible reactants' charge states, only excluding the condition where both Fe_i and H are positively charged, considering they are unlikely to bind due to the Coulombic repulsion. It is also possible that more than one combination of charge states of the reactants participates in the reaction. Such conditions are discussed in more detail below.

We calculate the charge states of Fe_i and H in silicon as a function of temperature and injection level applying the general occupancy factor described in Ref. 23. The assumptions and the parameters in the model are consistent with those in Ref. 23, but we use the temperature-dependent capture cross sections of the isolated Fe_i in this work, taken from Ref. 32.

B. The reaction rate constant $k(T)$

According to the results of Liu *et al.*, the dehydrogenation (the reaction in the opposite direction of hydrogenation, which is likely the thermal dissociation of the FeH complex) is not significant below 700 °C,[8] although we note that recent results[33] indicate that some forms of FeH complexes do

TABLE I. Possible reactants' charge states.

x	y	Reactants
0	+	$Fe^0 + H^+$
	0	$Fe^0 + H^0$
	−	$Fe^0 + H^-$
+	0	$Fe^+ + H^0$
	−	$Fe^+ + H^-$

[This article is copyrighted as indicated in the article. Reuse of AIP content is subject to the terms at: http://scitation.aip.org/termsconditions. Downloaded to] IP: 130.56.107.4 On: Wed, 28 Oct 2015 23:41:13

seem to dissociate at lower temperatures. Therefore, we neglect the dehydrogenation in this work (250 °C–700 °C). Applying the law of mass action to the reaction expressed by Eq. (1), at a fixed temperature T, we have

$$\frac{d[\mathrm{Fe_i}]}{dt} = -k(T)\cdot f(\mathrm{Fe}^x)\cdot f(\mathrm{H}^y)\cdot[\mathrm{Fe_i}][\mathrm{H}], \tag{2}$$

where $k(T)$ is the reaction rate constant; $f(\mathrm{Fe}^x)$ and $f(\mathrm{H}^y)$ are the fractions of the charge states Fe^x and H^y; and [H] is a steady-state concentration of monatomic hydrogen in the bulk.

During hydrogenation, the carrier distributions across the energy levels of isolated $\mathrm{Fe_i}$ and monatomic H both under thermal equilibrium (in the dark) or in steady state (under injection) are constantly being re-established. We assume that the time required for this process is negligible in comparison with the time constant of the hydrogenation reaction at each temperature. The result is that $f(\mathrm{Fe}^x)$ and $f(\mathrm{H}^y)$ are not subject to the consumption of the reactants by the hydrogenation but remain constant when the temperature and the injection conditions are fixed.

The monatomic hydrogen concentration N_H in the silicon bulk introduced by annealing the nitride films is a function of the annealing temperature T and the annealing time t. N_H is subject to many factors including, for example, the properties of the nitride film and the diffusion length of H.[31,34–37] After annealing at T for a long enough time, N_H will approximately achieve a steady state and will no longer change significantly.[36] We label the monatomic hydrogen concentration at this steady state as [H], which appears in Eq. (2), and assume that [H] is always larger in magnitude than $1\times10^{14}\,\mathrm{cm^{-3}}$ in the temperature range of 250 °C–700 °C.[35,36] The [$\mathrm{Fe_i}$] in the samples with the higher implantation dose is about $1\times10^{13}\,\mathrm{cm^{-3}}$, so this assumption ensures $[\mathrm{H}]\gg[\mathrm{Fe_i}]$. As a result, the hydrogen concentration [H] will not change significantly even if all the $\mathrm{Fe_i}$ atoms are passivated.

Therefore, the solution to Eq. (2) is an exponential reduction in [$\mathrm{Fe_i}$]

$$[\mathrm{Fe_i}] = N_t\cdot\exp\left[-k(T)f(\mathrm{Fe}^x)f(\mathrm{H}^y)[\mathrm{H}]\cdot t\right], \tag{3}$$

with N_t being the initial concentration of $\mathrm{Fe_i}$. The time constant is

$$\tau(T) = \frac{1}{k(T)}\cdot\frac{1}{f(\mathrm{Fe}^x)f(\mathrm{H}^y)}\cdot\frac{1}{[\mathrm{H}]}. \tag{4}$$

From Eq. (4), we know that with a fitted value of the time constant $\tau(T)$ from the experiments, the corresponding reaction rate constant can be calculated as

$$k(T) = \frac{1}{\tau(T)}\cdot\frac{1}{f(\mathrm{Fe}^x)f(\mathrm{H}^y)}\cdot\frac{1}{[\mathrm{H}]}. \tag{5}$$

C. Determination of the reactants' charge states

In Eq. (4), the reaction rate constant $k(T)$ and the monatomic hydrogen concentration [H] are reasonably assumed to be injection-independent. However, carrier injection does have effects on the fractions $f(\mathrm{Fe}^x)$, $f(\mathrm{H}^y)$, thus it will also impact the time constant $\tau(T)$. Comparing the hydrogenation reaction in thermal equilibrium and under injection of Δn, the ratio of the time constants is

$$\frac{\tau(T,\,\mathrm{thermal})}{\tau(T,\,\Delta n)} = \frac{\left[f(\mathrm{Fe}^x)f(\mathrm{H}^y)\right](T,\,\Delta n)}{\left[f(\mathrm{Fe}^x)f(\mathrm{H}^y)\right](T,\,\mathrm{thermal})}. \tag{6}$$

We label the ratio on the right of Eq. (6) as $r_{\mathrm{ff}}\,(\Delta n)$, and we can calculate it by assuming charge states for the reactants as shown in Table I. We found that there is considerable difference in the predicted ratios for different assumed reacting charge states. To determine the values of the left hand side of Eq. (6), we conduct the hydrogenation experiments in the dark and under injection. By comparing the experimental results and the modelling results, we are able to identify the reactants' charge states.

D. The activating energy E_a

The reaction rate constant $k(T)$ is governed by the activation energy E_a via the Arrhenius equation. At each investigated temperature T in the experiments, we have one or more fitted values of the time constant $\tau(T)$. The reaction rate constant $k(T)$ can be calculated by applying Eq. (5), where the only unknown parameter, is the monatomic hydrogen concentration [H]. However, the temperature-dependence of the monatomic hydrogen concentration is not easy to measure and is unavailable in the literature, so we assume it to be temperature-independent when determining the activation energy. Being aware that this assumption is not necessarily valid, we will discuss the effects of the possible temperature-dependence of [H] in greater detail in the sections below. Under the assumption that [H] is temperature-independent, we can fit

$$\frac{1}{\tau(T)}\times\frac{1}{f(\mathrm{Fe}^x)f(\mathrm{H}^y)} = Z\times\exp\left(-\frac{E_a}{k_BT}\right) \tag{7}$$

to obtain a value of the activation energy.

In the determination of the activation energy, the time constants measured in thermal equilibrium are used. Since the temperature range is now enlarged to 250 °C–700 °C, another method to determine the reactants' charge states is made possible, taking advantage of the temperature-dependence of $f(\mathrm{Fe}^x)$ and $f(\mathrm{H}^y)$. That is, for each pair of possible reacting charge states listed in Table I, a set of $\tau(T)^{-1}\cdot f(\mathrm{Fe}^x)^{-1}\cdot f(\mathrm{H}^y)^{-1}$ (the left side of Eq. (7)) in the temperature range of 250 °C–700 °C can be calculated and fitted to Eq. (7). The set of data assuming the actual reacting charge states should fit well, while improper assumptions of the reacting charge states could be expected to generate unreasonable fitting. This determines the reactants' charge states in an independent way from Section III C and meanwhile gives an estimation of the activation energy for the hydrogenation reaction.

[This article is copyrighted as indicated in the article. Reuse of AIP content is subject to the terms at: http://scitation.aip.org/termsconditions. Downloaded to] IP: 130.56.107.4 On: Wed, 28 Oct 2015 23:41:13

IV. RESULTS

A. Determination of the reactants' charge states

Figure 1 shows the modelling results of $f(Fe^x) \cdot f(H^y)$ as a function of carrier injection at 250 °C. Figure 2 shows $f(Fe^x) \cdot f(H^y)$ as a function of carrier injection at 300 °C. In comparison with 250 °C, a same injection level has less influence on the charge distributions, due to the increasing concentrations of the equilibrium carriers when elevating the temperature.[23] One can see from Figures 1 and 2 that $f(Fe^x) \cdot f(H^y)$ is always monotonic, either increasing or decreasing, no matter what reacting charge states are assumed. Therefore, we can use r_{ff} (Δn), which is the ratio on the right of Eq. (6), to quantify the injection-dependence of $f(Fe^x) \cdot f(H^y)$. It will approximate unity when $f(Fe^x) \cdot f(H^y)$ is almost independent of injection and deviate from unity when $f(Fe^x) \cdot f(H^y)$ is injection-dependent. Assuming different reacting charge states, there is a large difference between the values of r_{ff} (Δn). The predicted r_{ff} ($\Delta n = 2 \times 10^{16}\,cm^{-3}$) and r_{ff} ($\Delta n = 1 \times 10^{17}\,cm^{-3}$) at 250 °C and 300 °C are listed in Table II. These two special injection levels are chosen because in the experiments, we estimate the injection levels achieved in the samples under illumination to be in the range of 2×10^{16}–$5 \times 10^{16}\,cm^{-3}$ at the beginning of the annealing and above $1 \times 10^{17}\,cm^{-3}$ in the end (due to the increasing lifetime).

Figure 3 shows the experimental results at 250 °C. In the two samples with nitride films, the concentrations of Fe_i reduce exponentially, which confirms Eq. (3) in the modelling procedure. Within the uncertainty, there is effectively no change in $[Fe_i]$ in the oxide control sample, and we attribute this to the fact that there is no hydrogen. The comparison of the two samples with nitride films shows that the illumination makes a small but detectible difference on the kinetics of hydrogenation. The ratio of the time constant in the dark to that under illumination is 1.5, in the uncertainty range of 1.3–2.1. This value agrees best with the value of r_{ff} when

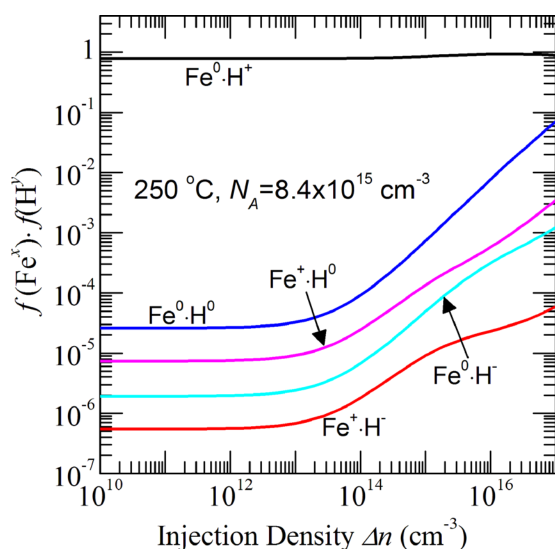

FIG. 1. The product of the fractions of Fe_i and H in possible reacting charge states, as a function of the injection density at 250 °C in p-Si with a doping of $8.4 \times 10^{15}\,cm^{-3}$.

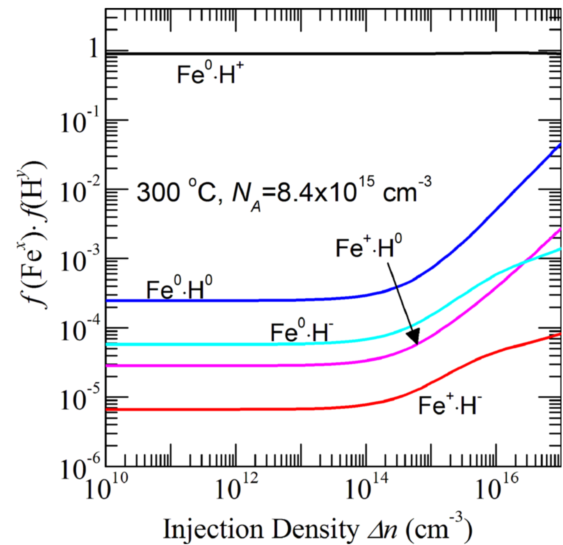

FIG. 2. The product of the fractions of Fe_i and H in possible reacting charge states, as a function of the injection density at 300 °C in p-Si with a doping of $8.4 \times 10^{15}\,cm^{-3}$.

assuming the reactants are Fe^0 and H^+, as shown in Table II. As measured by a thermocouple, the illumination may increase the sample temperature by up to 30 °C. However, even considering this possible uncertainty, based on the experimental and modelling results, other possible reacting charge states can still be ruled out.

A potential complication is that for p-Si with a doping of $8.4 \times 10^{15}\,cm^{-3}$, 250 °C is not high enough to dissociate all the FeB pairs in the dark. The fraction of FeB pairs in thermal equilibrium at 250 °C can be up to 15%.[29,38] However, in the illuminated sample, almost all the FeB pairs are dissociated by the injection, which is estimated to be above $2 \times 10^{16}\,cm^{-3}$.[23] We denote the measured concentration of Fe_i as $[Fe_i]_{measured}$. When we measure the concentration of Fe_i at room temperature, we are measuring the total Fe_i, using the lifetimes in the full associated state and in the fully dissociated state.[29] However, when we discuss the kinetics in the modelling procedure, the $[Fe_i]$ only includes the isolated Fe_i atoms that are able to pair with H. At 300 °C and above, almost all the FeB pairs will be dissociated even in the dark, so that $[Fe_i]_{measured} = [Fe_i]$. But at 250 °C, $[Fe_i]_{measured}$ is obviously higher than $[Fe_i]$, and $[Fe_i] = f_{diss} \cdot [Fe_i]_{measured}$, f_{diss} being the fraction of isolated Fe_i in thermal equilibrium. Combining this relation and Eq. (3), we have

TABLE II. r_{ff} ($\Delta n = 2 \times 10^{16}\,cm^{-3}$) and r_{ff} ($\Delta n = 1 \times 10^{17}\,cm^{-3}$) at 250 °C and 300 °C.

	250 °C		300 °C	
Reactants	$\Delta n = 2 \times 10^{16}\,cm^{-3}$	$\Delta n = 1 \times 10^{17}\,cm^{-3}$	$\Delta n = 2 \times 10^{16}\,cm^{-3}$	$\Delta n = 1 \times 10^{17}\,cm^{-3}$
$Fe^0 + H^+$	1.19	1.13	1.03	1.00
$Fe^0 + H^0$	587	2700	39.3	183
$Fe^0 + H^-$	244	630	13.6	24.0
$Fe^+ + H^0$	127	465	23.5	95.5
$Fe^+ + H^-$	52.6	109	8.16	12.6

[This article is copyrighted as indicated in the article. Reuse of AIP content is subject to the terms at: http://scitation.aip.org/termsconditions. Downloaded to] IP: 130.56.107.4 On: Wed, 28 Oct 2015 23:41:13

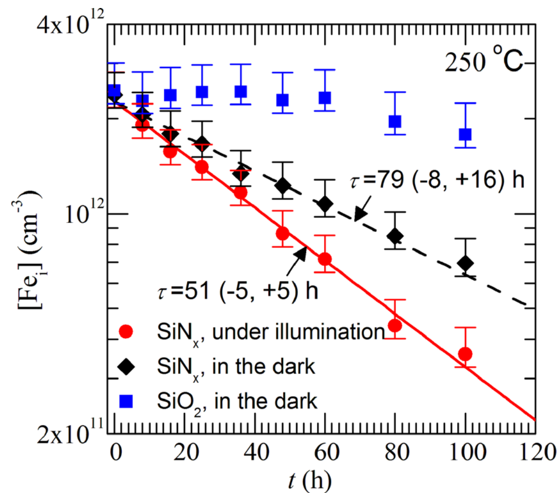

FIG. 3. $[Fe_i]$ as a function of cumulative annealing time at 250 °C, measured on a sample with SiO_2 film, a sample with SiN_x films in the dark, and a sample with SiN_x films under illumination.

$$[Fe_i]_{measured} = \frac{N_t}{f_{diss}} \times \exp\left[-k(T)f(Fe^x)f(H^y)[H] \times t\right]. \quad (8)$$

When the temperature and the doping level are fixed, the fraction f_{diss} is also fixed. Equation (8) indicates that $[Fe_i]_{measured}$ also reduces exponentially, having the same time constant with the reduction of $[Fe_i]$. Therefore, we can always fit $[Fe_i]_{measured}$ to determine the time constant of the reaction of $[Fe_i]$ even when there is only partial dissociation of FeB pairs at the annealing temperature in the dark.

Figure 4 shows the experimental results at 300 °C, including both sets of the experiments at this temperature. Again significant reductions in $[Fe_i]$ are observed in the samples with SiN_x films, and much slower reductions in the samples with SiO_2 films. As hydrogen is not present in the samples with oxide films, the reduction in $[Fe_i]$ should be caused by the precipitation at crystallographic defects, which may be introduced by the implantation or the annealing,[10,39] or occur at the surfaces. Comparing the two samples with SiO_2 films, we can see that the reduction in $[Fe_i]$ in the sample with a higher initial $[Fe_i]$ is more pronounced. This is expected as a higher initial $[Fe_i]$ increases the precipitation rate.[40] However, comparing the two samples with SiN_x films annealed in the dark, the time constants are within each other's uncertainty range. This further supports our model of the kinetics: first, we indeed observed exponential reductions in $[Fe_i]$ during the hydrogenation (Eq. (3)), and now we show that the time constant does not depend on the initial $[Fe_i]$ in the samples (Eq. (4)). This also indicates that the main reason for the reduction of [Fei] in the samples with nitride films should not be precipitation, otherwise the reduction would be faster with a higher initial [Fei].[40]

Comparing the two samples with lower initial $[Fe_i]$ with SiN_x films, again we did not observe a significant impact of the illumination. The ratio of the time constants is 1.2 in the range of 0.9–1.4. It also agrees the best with r_{ff} when assuming the reactants are Fe^0 and H^+ (Table II), in agreement with the conclusion from the experiments at 250 °C. Furthermore, although the uncertainty ranges of the ratios at 250 °C and 300 °C overlap, there is a slight reduction at 300 °C, in good agreement with the predicted trend. This indicates that the illumination has less impact on the charge distributions and thus the kinetics of hydrogenation when the concentrations of the equilibrium carriers are increased at higher temperatures.

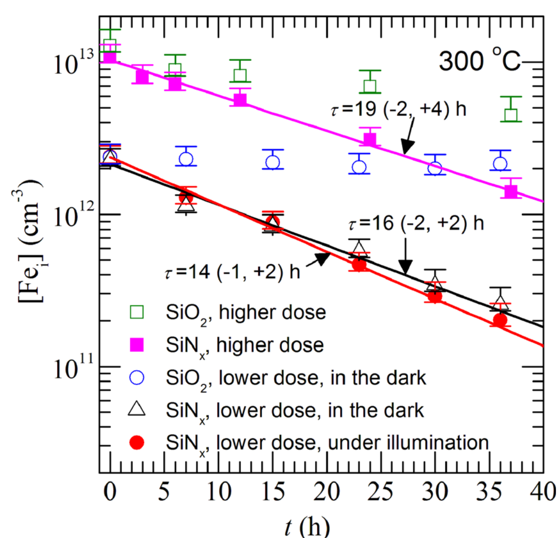

FIG. 4. $[Fe_i]$ as a function of cumulative annealing time at 300 °C. The two samples with higher initial $[Fe_i]$ were annealed in the dark, one with SiO_2 films and another with SiN_x films. Other three samples with lower initial $[Fe_i]$ were annealed with SiO_2 films in the dark, with SiN_x films in the dark and with SiN_x films under illumination, respectively.

B. The analysis of the activation energy

Figure 5 shows $[Fe_i]$ as a function of cumulative annealing time at 400 °C in the dark, measured on a sample with SiN_x films and a sample with SiO_2 films. The experimental results at 500 °C are shown in Figure 6, and the results at 600 °C and 700 °C are shown in Figure 7. At each temperature, there is a significant reduction in $[Fe_i]$ in the sample(s) with SiN_x films, but much slower or no reduction in the sample with SiO_2 film. For the samples with SiN_x films annealed

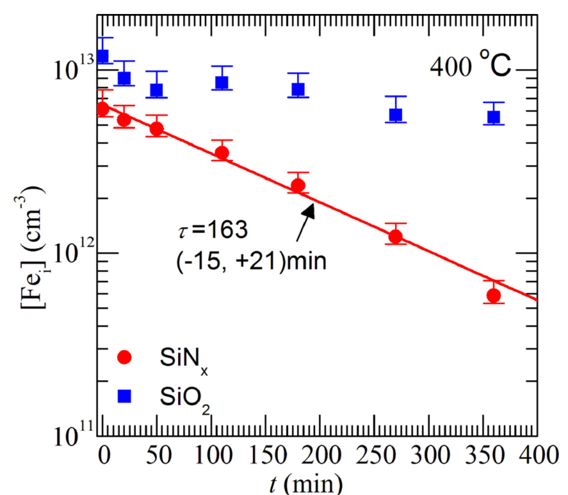

FIG. 5. $[Fe_i]$ as a function of cumulative annealing time at 400 °C in the dark, measured on a sample with SiO_2 films and a sample with SiN_x films.

[This article is copyrighted as indicated in the article. Reuse of AIP content is subject to the terms at: http://scitation.aip.org/termsconditions. Downloaded to] IP: 130.56.107.4 On: Wed, 28 Oct 2015 23:41:13

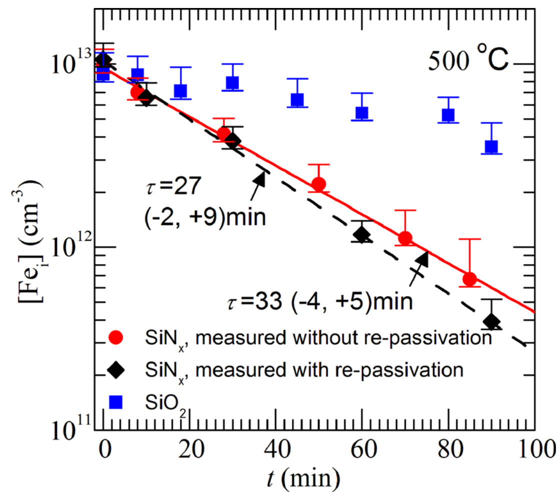

FIG. 6. $[Fe_i]$ as a function of cumulative annealing time at 500 °C in the dark, measured on a sample with SiO_2 films and two samples with SiN_x films. One of the samples with SiN_x films was re-passivated every time before measuring $[Fe_i]$, while the SiN_x films of the other sample were never changed during the experiments.

in the temperature range of 250 °C–400 °C, we did not change the nitride films during the experiments, as there was no obvious degradation of the surface passivation. However, we did observe significant degradation of the surface passivation when we annealed and measured a sample with SiN_x films at 500 °C. Note that although the surface passivation degraded, we still observed large difference between the lifetimes before and after dissociation of FeB pairs. This ensures that the uncertainties in the measured $[Fe_i]$ would not be significantly increased by the degraded surface passivation or lifetimes.[29] However, the degradation of the surface passivation may reflect a reduction in the amount of the monatomic H that is released by the nitride films and diffuses into the bulk of the wafers. So, we annealed another sample with SiN_x films at 500 °C, which was re-passivated with a fresh nitride film every time before we measured $[Fe_i]$. However, as shown in Figure 6, the difference between the kinetics measured on the two samples is minor; the time constants are within each other's uncertainty range. This means the amount of monatomic H that diffuses into the bulk is not significantly affected by the degradation of the surface passivation in the investigated period. It is also a hint that at the lower temperature range where the surface passivation does not degrade obviously, the amount of monatomic H in the bulk should be quite constant. At 600 °C and 700 °C, the nitride film degrades more seriously, so it was necessary to re-passivate the samples every time before measuring $[Fe_i]$.

Figure 8 shows the modelling results of $f(Fe^x) \cdot f(H^y)$ as a function of temperature in thermal equilibrium. Corresponding to the possible reacting charge states listed in Table I, five sets of $\tau(T)^{-1} \cdot f(Fe^x)^{-1} \cdot f(H^y)^{-1}$ as a function of 1000/T are shown in Figure 9. Figure 9(a) shows the results when assuming the reactants are $Fe^+ + H^-$, $Fe^+ + H^0$, $Fe^0 + H^-$, and $Fe^0 + H^0$. Obviously, none of these four sets of data can be reasonably fitted on a straight line. The best fitting is observed when assuming the reactants are $Fe^0 + H^+$, shown in Figure 9(b). This is in agreement with the previous conclusion on the reactants' charge states. The fitted value of E_a given by this set of data is 0.76 eV.

V. DISCUSSION

A. Hydrogen passivation of Fe_i

Figure 10 shows the lifetime at $\Delta n = 1 \times 10^{15}\,cm^{-3}$ in both the fully associated state and the fully dissociated state, as a function of $[Fe_i]$, measured on the samples with SiN_x films. The only sample excluded was that annealed at 500 °C and measured without re-passivation, as we observed obvious degradation of the surface passivation on this sample. The data points at $[Fe_i] = 1 \times 10^{13}\,cm^{-3}$ in the fully associated state are missing because the lifetimes were too low for an injection level of $1 \times 10^{15}\,cm^{-3}$ to be achieved during the measurement. The data points are fitted to a reciprocal relation that $\tau_{eff} \cdot [Fe_i] = $ constant. The data points with the lowest concentrations of Fe_i, which do not fit so well

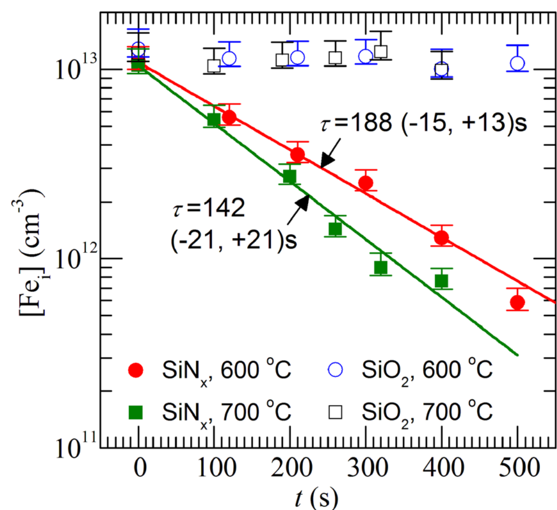

FIG. 7. $[Fe_i]$ as a function of cumulative annealing time at 600 °C and 700 °C in the dark, measured on a sample with SiO_2 films and a sample with SiN_x films at each temperature.

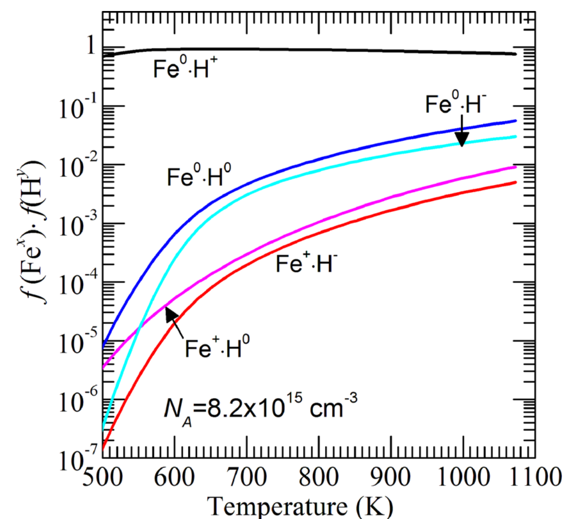

FIG. 8. The product of the fractions of Fe_i and H in possible reacting charge states, as a function of temperature in thermal equilibrium in p-Si with a doping of $8.2 \times 10^{15}\,cm^{-3}$.

[This article is copyrighted as indicated in the article. Reuse of AIP content is subject to the terms at: http://scitation.aip.org/termsconditions. Downloaded to] IP: 130.56.107.4 On: Wed, 28 Oct 2015 23:41:13

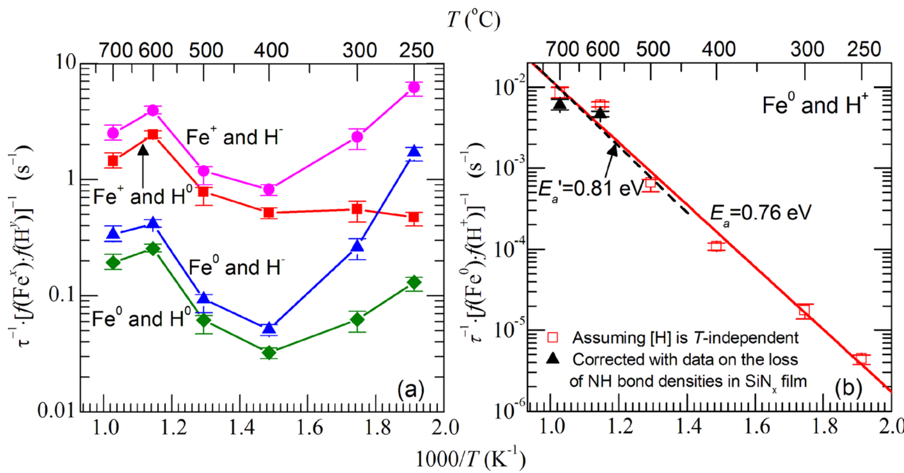

FIG. 9. $\tau(T)^{-1}\cdot f(Fe^x)^{-1}\cdot f(H^y)^{-1}$ as a function of 1000/*T*, assuming the reacting charge states to be (a) $Fe^+ + H^-$, $Fe^+ + H^0$, $Fe^0 + H^-$, $Fe^0 + H^0$ and (b) $Fe^0 + H^+$. In (b), the data points corrected with the data on the loss of NH bond densities in SiN_x films upon annealing and the fitting are also shown.

with the straight lines, are mainly measured on the samples with a lower implantation dose annealed at 300 °C. On these samples, we passivated Fe_i until such low concentrations were reached that the degradation of the surface passivation becomes obvious on this plot. Except for these points, the data fit well with the reciprocal relations. This means that (a) the lifetimes of the samples are always dominated by isolated Fe_i or FeB pairs and (b) no other recombination centres, which are comparably as strong as isolated Fe_i or FeB pairs, are created during the reaction. This agrees with the hypothesis that the reduction in $[Fe_i]$ is caused by the paring of Fe_i and H, forming a recombination-inactive hydride complex.[5,8]

In the recent experiments of Liu *et al.*,[8] the samples at 600 °C and 700 °C were annealed for long enough that Fe_i was passivated to concentrations below the solubility limit. This is a solid evidence that the observed reductions in $[Fe_i]$ at 600 °C and 700 °C are not caused by precipitation.[8] In this work, we hydrogenated Fe_i by applying the same method in the temperature range of 250 °C–700 °C. In Figure 9(b), we showed that assuming reasonable reacting charge states, all the data points can fit well on the same straight line, indicating the same thermally activated behaviour at all temperatures. We regard the hydrogen passivation of Fe_i, namely, the pairing of Fe_i and H forming a recombination-inactive hydride, as the most probable explanation, which successfully explains the different behaviours of Fe_i in the samples with SiN_x films and SiO_2 films, the exponential reductions of $[Fe_i]$ (as shown in Figures 3–7), and also the similar time constants when the initial $[Fe_i]$ varies (Figure 4). However, despite these positive evidences, we cannot absolutely exclude the possibility that an accelerated precipitation of Fe due to the presence of hydrogen may affect the results.

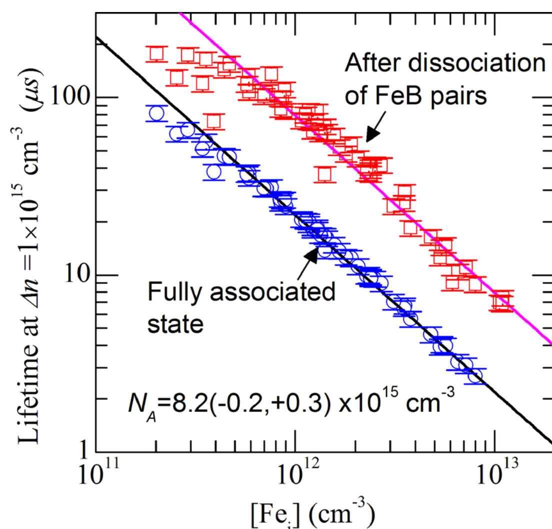

FIG. 10. The lifetime at $\Delta n = 1\times10^{15}\,cm^{-3}$ as a function of the Fe_i concentration, fitted to reciprocal relations. Except the sample with SiN_x films annealed at 500 °C without re-passivation, all the data measured on samples with SiN_x films are included.

B. The reactants' charge states in the hydrogenation of Fe_i

In the results, Fe^0 and H^+ are identified as the reacting charge states. However, as shown in the modelling results in Figures 1, 2, and 8, for the whole investigated injection and temperature range, Fe^0 always has a much higher concentration than Fe^+ and H^+ always has a much higher concentration than H^0 and H^-. A potential ambiguity is that, when the majority charge states participate in the reaction, whether the minority charge states also participate or not will have no effect on the measurements, due to their much lower concentrations. Based on the current results, we can therefore only conclude that the reaction is dominated by the reactants Fe^0 and H^+; whether other charge states also react cannot be determined.

Interestingly, in comparison with the permanent deactivation of BO defects where the role of illumination is found to be crucial, we found that illumination does not have a significant impact on the hydrogenation of Fe_i. This can be explained by the difference between the two defects and between the reacting charge states of H, assuming that the permanent deactivation of the BO defect is indeed caused by hydrogenation. For BO defects, the illumination is vital to keep them activated at elevated temperatures so that the permanently deactivated state can be achieved.[12] Otherwise, if the BO defects are annealed in the dark, they will be dissociated and can never directly convert to the permanently deactivated state.[12] This is the most important reason why the illumination is required in the process. The role of

[This article is copyrighted as indicated in the article. Reuse of AIP content is subject to the terms at: http://scitation.aip.org/termsconditions. Downloaded to] IP: 130.56.107.4 On: Wed, 28 Oct 2015 23:41:13

illumination is further emphasized by the models recognising the importance of H^0 in passivating the BO defects.[19,20,25] As predicted, the injection can increase the fraction of H^0 in the temperature range that BO defects are passivated, in both p-Si and compensated n-Si.[23] However, in the case of Fe_i, the illumination barely makes any difference on the defect itself or the fractions of the dominating reacting charge states Fe^0 and H^+. As a result, the illumination is found to have much less significant influence on the hydrogenation of Fe_i.

Since we concluded that Fe^0 and H^+ are reacting in the hydrogenation, the reaction is then not driven by the Coulombic attraction, and the bond between Fe_i and H should not be an ionic bond. This is also the case in the passivation of BO defects if H^0 is the reacting charge state.[20] In addition, some recent results showed the long-time stability of the permanent deactivation of BO defects in compensated n-Si.[22,24] Combining the modelling results of the charge states, the authors attributed the binding of H and BO defects to covalent binding rather than an ionic interaction.[22]

C. The effects of the temperature-dependence of [H]

We assumed [H] to be temperature-independent in the determination of the activation energy, but in this large temperature range of 250 °C–700 °C, one may reasonably expect a variation in [H]. However, as clarified before, [H] is the steady-state concentration of hydrogen. To achieve this steady state, it takes tens of seconds at 750 °C[36] but may take hours at 200 °C–300 °C according to the diffusivity of hydrogen.[35,37] In our experiments, the average annealing time interval is 80 s at 700 °C, 100 s at 600 °C, 20 min at 500 °C, 1 h at 400 °C, 7.2 h at 300 °C, and 12.5 h at 250 °C. At each temperature, this interval is comparable in scale with the time length to achieve the steady-state [H]. This ensures that we mostly measured the kinetics after achieving the steady state. It also clarifies that we are not assuming the same hydrogen concentration at different temperatures after annealing the nitride films for the same time. On the contrary, the assumption indicates that to achieve a similar hydrogen concentration, one may have to anneal the nitride film for a time orders of magnitudes longer at 250 °C than 700 °C.

The second method to determine the reactants' charge states relies heavily on this assumption. However, the data points in Figure 9(a) distribute quite randomly, which is unlikely to be caused by the temperature-dependence of [H]. For example, for $Fe^+ + H^-$ and $Fe^0 + H^-$, the highest values of $\tau(T)^{-1} \cdot f(Fe^x)^{-1} \cdot f(H^y)^{-1}$ are both observed at 250 °C, and the lowest values are at 400 °C. If the activation energy has a positive value, [H] at 250 °C has to be orders of magnitudes higher than that at 400 °C, which is very unlikely to be the case. In addition, the first method to determine the reactants' charge states does not rely on this assumption, and the same reacting charge states are concluded with much less uncertainty. Therefore, the assumption of the temperature-independence of [H] will not affect our conclusion on the reacting charge states.

However, this assumption may impact the value of the activation energy. Boehme and Lucovsky[41] measured the evolution of the NH area bond densities during annealing remote PECVD silicon nitride films. For the SiN_x, which is the most similar to ours, the lost fractions of NH bond densities after annealing at 500 °C for 800 s, 600 °C for 100 s, and 700 °C for 80 s are about 0.25, 0.34, and 0.35, respectively.[41] They only measured the data at 500 °C up to 800 s, so we use 800 s instead of 20 min at this temperature; but as seen from the trend of the curve, the fraction at 20 min should be a little higher than 0.25 and closer to the fraction 0.34 at 600 °C.[41] Most of the loss of the NH bonds is caused by two competing mechanisms: the formation of H_2 and the release of monatomic H.[41–43] The monatomic H that diffuses into the bulk of silicon and passivates the defect is mainly generated by the second mechanism.[34,36,41,42] The competition of the two mechanisms mainly depends on the density of the nitride film: a film with a lower density favours the formation of H_2, while a higher density favours the release of H.[34,42] We make another assumption here that the competition is not dependent on the annealing temperature, so that at different temperatures, the fraction of the monatomic H, which diffuses into the bulk, remains the same. This is not necessarily valid, but it helps narrow down the variables. Under this assumption, we correct $\tau(T)^{-1} \cdot f(Fe^x)^{-1} \cdot f(H^y)^{-1}$ using the data on the lost fractions of NH bond densities from Ref. 41 to account for the temperature-dependence of [H] in the model. The corrected data at 600 °C and 700 °C when assuming [H] at 500 °C is unity are shown in Figure 9(b). The fitted value of $E_a' = 0.81$ eV given by the corrected data at 500 °C–700 °C does not change much from the original value 0.76 eV. What is notable is that based on the data of Boehme *et al.*, the loss of NH bonds slightly increases as the temperature increases; as a result, fitting the corrected data should generate a lower value of E_a' than the original value. We attribute the higher E_a' to the uncertainties in the data points at 500 °C–700 °C and the uncertainties associated with the fitting. The most probable value of the activation energy is estimated to be in the 0.7–0.8 eV range.

VI. CONCLUSIONS

In this work, we annealed Fe-containing samples with SiN_x films and SiO_2 films in the temperature range of 250 °C–700 °C, and significant reductions in [Fe_i] were only observed in the samples with SiN_x films. We rule out the precipitation of Fe_i as the reason for the reductions. We propose the hydrogen passivation of Fe_i, which is the complexing of monatomic H and isolated Fe_i forming a recombination-inactive hydride, as the most probable model to explain the reductions. Under this hypothesis, good agreement is observed between the model and the experimental results on the kinetics of the reaction.

We determined the reactants' charge states in two different ways: (a) By examining the effect of illumination on the kinetics of the reaction at 250 °C and 300 °C, and taking advantage of the injection-dependence of the charge distributions on the Fe_i and H levels; (b) By fitting the reaction kinetics in a large temperature range of 250 °C–700 °C with the Arrhenius equation, and taking advantage of the temperature-dependence of the charge distributions. In the

[This article is copyrighted as indicated in the article. Reuse of AIP content is subject to the terms at: http://scitation.aip.org/termsconditions. Downloaded to] IP: 130.56.107.4 On: Wed, 28 Oct 2015 23:41:13

first method, the illumination is found to have a small but detectible impact on the kinetics. This is attributed to the dominating reacting charge states Fe^0 and H^+, which are the majority charge states of isolated Fe_i and monatomic H, and thus their fractions are not strongly injection-dependent. The second method supports the conclusion on the dominating reacting charge states $Fe^0 + H^+$ and gives a value of the activation energy of hydrogenation of 0.76 eV. Considering the temperature-dependence of the hydrogen concentration, we estimate the most probable value of the activation energy to be in the 0.7–0.8 eV range.

ACKNOWLEDGMENTS

This work has been supported through the Australian Renewable Energy Agency (ARENA) through their fellowship program, project RND009, and the Australian Centre for Advanced Photovoltaics. Support from the Australian Research Council (ARC) Future Fellowships program is also acknowledged.

[1]K. Graff, *Metal Impurities in Silicon-Device Fabrication* (Springer, Berlin, 2000).
[2]A. A. Istratov, T. Buonassisi, R. McDonald, A. Smith, R. Schindler, J. Rand, J. P. Kalejs, and E. R. Weber, J. Appl. Phys. **94**, 6552 (2003).
[3]D. Macdonald, A. Cuevas, A. Kinomura, Y. Nakano, and L. Geerligs, J. Appl. Phys. **97**, 033523 (2005).
[4]S. McHugo, H. Hieslmair, and E. Weber, Appl. Phys. A **64**, 127 (1997).
[5]M. Kouketsu and S. Isomae, J. Appl. Phys. **80**, 1485 (1996).
[6]L. J. Geerligs, A. Azzizi, D. H. Macdonald, and P. Manshanden, in *13th Workshop on Crystalline Silicon Solar Cell Materials and Processes, Vail, Colorado, 2003* (National Renewable Energy Laboratory, Golden, Colorado, 2004), pp. 199–202.
[7]K. McLean, C. Morrow, and D. Macdonald, in *4th World Conference on Photovoltaic Energy Conversion, Waikoloa, 2006* (IEEE, New York, 2006), Vol. 1, pp. 1122–1125.
[8]A. Liu, C. Sun, and D. Macdonald, J. Appl. Phys. **116**, 194902 (2014).
[9]P. Karzel, A. Frey, S. Fritz, and G. Hahn, J. Appl. Phys. **113**, 114903 (2013).
[10]R. Krain, S. Herlufsen, and J. Schmidt, Appl. Phys. Lett. **93**, 152108 (2008).
[11]A. Herguth, G. Schubert, M. Kaes, and G. Hahn, in *Proceedings of the 32nd IEEE PVSC (4th WCPEC), Waikoloa, USA* (2006), p. 940.
[12]A. Herguth, G. Schubert, M. Käs, and G. Hahn, Prog. Photovoltaics **16**, 135 (2008).
[13]G. Krugel, W. Wolke, J. Geilker, S. Rein, and R. Preu, Energy Procedia **8**, 47 (2011).
[14]K. Münzer, in *Proceedings of the 24th European Photovoltaic Solar Energy Conference, Hamburg* (2009), pp. 1558–1561.
[15]B. J. Hallam, S. R. Wenham, P. G. Hamer, M. D. Abbott, A. Sugianto, C. E. Chan, A. M. Wenham, M. G. Eadie, and G. Xu, Energy Procedia **38**, 561 (2013).
[16]S. Wilking, S. Ebert, A. Herguth, and G. Hahn, J. Appl. Phys. **114**, 194512 (2013).
[17]S. Wilking, A. Herguth, and G. Hahn, J. Appl. Phys. **113**, 194503 (2013).
[18]B. J. Hallam, P. G. Hamer, S. R. Wenham, M. D. Abbot, A. Sugianto, A. M. Wenham, C. E. Chan, G. Q. Xu, J. Kariem, J. Degoulange, and R. Einhaus, IEEE J. Photovoltaics **4**, 88 (2014).
[19]P. Hamer, B. Hallam, S. Wenham, and M. Abbott, IEEE J. Photovoltaics **4**, 1252 (2014).
[20]S. Wilking, C. Beckh, S. Ebert, A. Herguth, and G. Hahn, Sol. Energy Mater. Sol. Cells **131**, 2 (2014).
[21]N. Nampalli, B. Hallam, C. Chan, M. Abbott, and S. Wenham, Appl. Phys. Lett. **106**, 173501 (2015).
[22]S. Wilking, M. Forster, A. Herguth, and G. Hahn, "From simulation to experiment: Understanding BO-regeneration kinetics," Sol. Energy Mater. Sol. Cells (to be published).
[23]C. Sun, F. E. Rougieux, and D. Macdonald, J. Appl. Phys. **117**, 045702 (2015).
[24]T. Niewelt, J. Broisch, J. Schön, J. Haunschild, S. Rein, W. Warta, and M. C. Schubert, "Light-induced degradation and regeneration in n-type silicon," Energy Procedia (to be published).
[25]M. Gläser and D. Lausch, "Towards a quantitative model for BO regeneration by means of charge state control of hydrogen," Energy Procedia (to be published).
[26]B. Lim, "Boron–oxygen-related recombination centers in crystalline silicon and the effects of dopant-compensation," Ph.D. dissertation (University of Hannover, 2012).
[27]R. A. Sinton, A. Cuevas, and M. Stuckings, *Quasi-Steady-State Photoconductance: A New Method for Solar Cell Material and Device Characterization* (IEEE, New York, 1996), pp. 457–460.
[28]H. Nagel, C. Berge, and A. G. Aberle, J. Appl. Phys. **86**, 6218 (1999).
[29]D. Macdonald, L. Geerligs, and A. Azzizi, J. Appl. Phys. **95**, 1021 (2004).
[30]D. Macdonald, J. Tan, and T. Trupke, J. Appl. Phys. **103**, 073710 (2008).
[31]S. Pearton, J. Corbett, and T. Shi, Appl. Phys. A **43**, 153 (1987).
[32]B. Paudyal, K. McIntosh, and D. Macdonald, in 34th IEEE Photovoltaic Specialists Conference (PVSC) (IEEE, Philadelphia, 2009), p. 001588.
[33]S. Leonard, V. Markevich, A. Peaker, B. Hamilton, and J. Murphy, Appl. Phys. Lett. **107**, 032103 (2015).
[34]H. Dekkers, S. De Wolf, G. Agostinelli, F. Duerinckx, and G. Beaucarne, Sol. Energy Mater. Sol. Cells **90**, 3244 (2006).
[35]S. Kleekajai, F. Jiang, M. Stavola, V. Yelundur, K. Nakayashiki, A. Rohatgi, G. Hahn, S. Seren, and J. Kalejs, J. Appl. Phys. **100**, 093517 (2006).
[36]M. Sheoran, D. S. Kim, A. Rohatgi, H. Dekkers, G. Beaucarne, M. Young, and S. Asher, in *33rd IEEE Photovoltaic Specialists Conference (PVSC)* (IEEE, San Diego, 2008), p. 1.
[37]D. Mathiot, Phys. Rev. B **40**, 5867 (1989).
[38]L. Kimerling and J. Benton, Physica B+C **116**, 297 (1983).
[39]W. B. Henley and D. A. Ramappa, J. Appl. Phys. **82**, 589 (1997).
[40]A. Liu and D. Macdonald, J. Appl. Phys. **115**, 114901 (2014).
[41]C. Boehme and G. Lucovsky, J. Vac. Sci. Technol. A **19**, 2622 (2001).
[42]H. Dekkers, "Study and optimization of dry process technologies for thin crystalline silicon solar cell manufacturing," Ph.D. dissertation (Katholieke University of Leuven, Leuven, Belgium, 2008).
[43]H. Dekkers, G. Beaucarne, M. Hiller, H. Charifi, and A. Slaoui, Appl. Phys. Lett. **89**, 211914 (2006).

[This article is copyrighted as indicated in the article. Reuse of AIP content is subject to the terms at: http://scitation.aip.org/termsconditions. Downloaded to] IP: 130.56.107.4 On: Wed, 28 Oct 2015 23:41:13